

# PCCP

Accepted Manuscript



This is an *Accepted Manuscript*, which has been through the Royal Society of Chemistry peer review process and has been accepted for publication.

*Accepted Manuscripts* are published online shortly after acceptance, before technical editing, formatting and proof reading. Using this free service, authors can make their results available to the community, in citable form, before we publish the edited article. We will replace this *Accepted Manuscript* with the edited and formatted *Advance Article* as soon as it is available.

You can find more information about *Accepted Manuscripts* in the [Information for Authors](#).

Please note that technical editing may introduce minor changes to the text and/or graphics, which may alter content. The journal's standard [Terms & Conditions](#) and the [Ethical guidelines](#) still apply. In no event shall the Royal Society of Chemistry be held responsible for any errors or omissions in this *Accepted Manuscript* or any consequences arising from the use of any information it contains.

Molecular Structure and Thermal Stability of Oxide-Supported  
Phosphotungstic Wells-Dawson Heteropolyacid

Silvana R. Matkovic<sup>a</sup> Sebastián E. Collins<sup>b</sup>, Adrián L. Bonivardi<sup>b</sup>,  
Miguel A. Bañares<sup>c</sup>, Laura E. Briand<sup>a\*</sup>,

<sup>a</sup> Centro de Investigación y Desarrollo en Ciencias Aplicadas –Dr Jorge J. Ronco CINDECA-CCT La Plata-CONICET. Calle 47 No 257, B1900AJK, La Plata, Buenos Aires, Argentina.

<sup>b</sup> Instituto de Desarrollo Tecnológico para la Industria Química (UNL-CONICET). Güemes 3450, S3000GLN, Santa Fe, Argentina.

<sup>c</sup> Catalytic Spectroscopy Laboratory, ICP-CSIC. Marie Curie 2, E-28049 Madrid, Spain.

---

\* Corresponding author: briand@quimica.unlp.edu.ar Tel. 54 221 4 211353/210711.

**Abstract**

We present, for the first time in literature, a systematic study of the molecular structure of the Wells-Dawson heteropolyacid  $\text{H}_6\text{P}_2\text{W}_{18}\text{O}_{62}\cdot 24\text{H}_2\text{O}$  (HPA) dispersed on  $\text{TiO}_2$ ,  $\text{SiO}_2$ ,  $\text{ZrO}_2$  and  $\text{Al}_2\text{O}_3$ .

The heteropolyacid-based materials were synthesized through a conventional impregnation method (in aqueous and ethanol media) at a loading that corresponds to the theoretical “monolayer” coverage (dispersion limit loading). The combination of Raman and infrared studies demonstrates the presence of crystals of HPA (regardless of the nature of the medium used during the synthesis) suggesting that the dispersion limit loading was greatly exceeded.

*In situ* temperature programmed analyses demonstrated that the Raman shift of the distinctive  $\text{W}=\text{O}$  Raman mode of the phosphotungstic Wells-Dawson heteropolyacid is sensitive to the local environment, that is the amount of water molecules associated with the structure. Moreover, the aqueous based species associated with such structures are recognizable through infrared spectroscopy.

**Keywords:** Heteropolyacid, Wells-Dawson, Phosphotungstic, TP-IR *in situ*, TP-Raman *in situ*, Molecular Spectroscopy.

## 1. Introduction

Intense investigations reported in the past few years demonstrated the capability of several hetero-polyoxometalates - POMs - mainly of the Keggin and Wells-Dawson, to catalyze a variety of reactions in the liquid and in the gas phase<sup>1</sup>. Particularly, bulk and silica-supported phosphotungstic Wells-Dawson heteropolyacid  $H_6P_2W_{18}O_{62} \cdot 24H_2O$  (at the theoretical “monolayer” coverage) have proved to be active in the synthesis of organic substrates carried in heterogeneous fashion (solid catalyst and reactants in the liquid phase) with and without co-solvents and mild conditions. Recent advances in such field are the synthesis of substituted cumarins<sup>2</sup>, the esterification of levulinic acid with ethanol<sup>3</sup>, the cyclodehydration reaction of 1-(2-hydroxyphenyl)-3-phenyl-1,3-propanedione to obtain flavones<sup>4</sup>, among others.

Those HPA-catalyzed reactions might have been produced through one of the following mechanisms: conventional surface-type, pseudo-liquid bulk type and bulk-type catalysis<sup>5</sup>. The pseudo-liquid type of catalytic reaction occurs at the surface and within the structure of the POMs (three-dimensional fashion) due to the diffusion of the molecules (reactants and products) in-and-out of the secondary structure of the catalytic material. The heteropoly-compound must have an open and flexible structure for this mechanism to proceed, which in turn is tuned by the hydration degree and also the type of counteraction<sup>5</sup>.

The dependency of the degree of hydration with the temperature and its relevance in the pseudo-liquid and surface type catalysis of the phosphotungstic Wells-Dawson heteropolyacid was thoroughly investigated by Sambeth et al.<sup>6,7</sup>

and Micek-Ilnicka et al.<sup>8</sup>. The former demonstrated that the presence of the  $H_5O_2^+$  species bonded to the secondary structure of the HPA is essential for the catalytic process. Additionally, theoretical calculations indicate that the nature of the reactants influences the mechanism involved in the HPA's catalysis. In this context, Sambeth et al. concluded that polar substrates such as, methanol and diacetates conduct to a pseudo-liquid type of mechanism due to their ability to interact with the dioxonium aqueous  $H_5O_2^+$  species. Previously Micek-Ilnicka et al. studied the reaction of ethanol and isobutene over the phosphotungstic Wells-Dawson heteropolyacid  $H_6P_2W_{18}O_{62} \cdot xH_2O$  with various degree of hydration that is,  $x = 3, 8$  and zero (completely dehydrated). Their investigations on the HPA's adsorption capability of ethanol demonstrated that the higher the amount of crystallization water molecules the higher the amount of alcohol adsorbed and also higher catalytic activity of the material<sup>8</sup>.

Oxide-supported phosphotungstic Wells-Dawson HPA is actively used in various organic syntheses. Typically, the HPA is dispersed at the "theoretical monolayer coverage" loading, which is calculated as an average between the areas of the HPA with the elliptic and circular projections as will be discussed later. The term of "monolayer coverage" is normally used on supported systems to describe the dispersion limit loading, below which, species will be molecularly dispersed and interacting with the support. Segregated crystalline phases develop above such loading. In this context, literature shows that the dispersion limit loading of the Wells-Dawson HPA over silica with a surface area equals to  $250 \text{ m}^2\text{g}^{-1}$  would result in a material containing  $17 W_{\text{atoms}}/\text{nm}^2$  (tungsten atoms per  $\text{nm}^2$  of oxide support)<sup>9</sup>. Bielański et al. also extensively investigated silica

and titania supported catalysts at various loadings<sup>10</sup>. The HPA was dispersed in ethanol medium over the oxides supports in the 5-25 wt. % range corresponding to 1 to 11  $W_{\text{atoms}}/\text{nm}^2$  for  $\text{TiO}_2$  and 0.3 to 3  $W_{\text{atoms}}/\text{nm}^2$  for  $\text{SiO}_2$ . The authors demonstrated the presence of nanocrystals of the HPA over the oxide supports.

More recently Matkovic et al.<sup>11</sup> reported the molecular structure of Wells-Dawson HPAs dispersed over titania at various loadings (below and above the theoretical “monolayer” coverage) through *in situ* Raman and infrared spectroscopies. That investigation demonstrated that the real dispersion limit loading of the Wells-Dawson heteropolyacid  $\text{H}_6\text{P}_2\text{W}_{18}\text{O}_{62}\cdot 24\text{H}_2\text{O}$  on  $\text{TiO}_2$  is around  $2.2 \text{ Wnm}^{-2}$  according to the experimental evidences.

That investigation allowed to conclude that the amount of HPA for a full surface coverage calculated with the theoretical measurements of the Wells-Dawson phosphotungstic heteropolyanion  $\text{P}_2\text{W}_{18}\text{O}_{62}^{6-}$ , was actually far above the maximum dispersion limit to form a bi-dimensional layer over the oxide support.

The present investigation extends those findings in order to assess the actual molecular structure of the Wells-Dawson phosphotungstic HPA when dispersed over transition metal oxide supports. In addition, we addressed the influence of the nature of the synthesis media (aqueous vs. organic) and the degree of hydration on the molecular structure combining Raman and infrared spectroscopies under *in situ* conditions.

## 2. Experimental

### 2.1. Synthesis of the Heteropolyacid Dispersed on the Oxide Supports at Theoretical “Monolayer Coverage”

The phosphotungstic Wells-Dawson heteropolyacid  $H_6P_2W_{18}O_{62} \cdot xH_2O$  (HPA for brevity) was synthesized through ion exchange of the phosphotungstic salt  $(NH_4)_6P_2W_{18}O_{62} \cdot 13H_2O$  with an ion exchange resin<sup>12,13</sup>. Then, the heteropolyacid was dispersed over  $TiO_2$  (Aeroxide® P-18 Evonik Ind.,  $46.8 \pm 0.1 \text{ m}^2/\text{g}$ ),  $SiO_2$  (Cab-O-Sil,  $328.9 \pm 0.8 \text{ m}^2/\text{g}$ ),  $Al_2O_3$  (Engelhard,  $95.8 \pm 0.2 \text{ m}^2/\text{g}$ ) and  $ZrO_2$  (fumed Evonik Ind.,  $31.5 \pm 0.4 \text{ m}^2/\text{g}$ ) through conventional incipient wetness impregnation at 298 K overnight. The impregnation of the HPA over  $TiO_2$ ,  $Al_2O_3$ ,  $ZrO_2$  and  $SiO_2$  was performed by dissolving the appropriate amount of heteropolyacid either in distilled water or absolute ethanol (Merck, 99.8 %) in order to investigate the influence of the nature of the medium in the synthesis. The samples were dried at 373 K for 1 h and calcined at 573 K for 4 h.

The materials synthesized in the present investigation correspond to the theoretical dispersion limit loading of tungsten atoms per  $\text{nm}^2$  (the so called *monolayer coverage*) according to geometric considerations i.e., 1.57 HPA molecules per  $\text{nm}^2$  of oxide support<sup>6, 14</sup>. The amount of HPA required to reach a full surface coverage was calculated considering an elliptical projection of the HPA over the metal oxide support.

Hereafter, each catalyst is named with the value of tungsten atoms per  $\text{nm}^2$  of oxide support ( $W_{\text{atoms}}/\text{nm}^2$ ) of the Wells Dawson “WD” heteropolyacid,

followed by the indication “aq” or “org” for aqueous or organic synthesis respectively and the indication of the support. Therefore the materials are: 11aq WDTi, 11org WDTi, 11aq WZr, 11org WZr, 12aq WDAI, 12org WDAI and 11aq WDSi. The X-ray diffraction analysis of these materials is presented in the Supplementary Information section.

The specific surface area of these samples was determined through the conventional BET method with a Micromeritics ASAP 2020 equipment.

### 2.2. *In Situ Temperature Programmed Raman Spectroscopy*

Raman spectra were collected using a single monochromator Renishaw System 1000 equipped with a thermoelectrically cooled CCD detector (200 K) and an edge filter. A laser of 514 nm Ar line was used and the spectral resolution was 3  $\text{cm}^{-1}$  and 0.9 mW laser power on sample. The Raman spectrometer was equipped with an *in situ* environmental cell (Linkam TS-1500) where both the temperature and the gaseous composition were controllable. Initially, the spectra of the samples were taken at room temperature. Then, the materials were maintained at 373 K for 1500 sec and further heated to 773 K at 10 K/min under an atmosphere of high purity grade He (99.999%) at 30  $\text{cm}^3/\text{min}$ , as reported elsewhere<sup>11, 15</sup>. The spectra were taken every 50 K along the temperature ramp.

### 2.3. *In Situ Temperature Programmed Infrared Spectroscopy*

The supported materials were investigated by *in situ* transmission infrared spectroscopy on self-supported wafers placed into a heated glass cell fitted with NaCl windows and attached to high vacuum system (base pressure =  $1.33 \times 10^{-4}$  Pa) and manifold for gas flow operation, as described previously<sup>16</sup>.

The stability and the hydration state of the supported HPA were studied by collecting *in situ* IR spectra during its heating from RT to 723 K at  $10 \text{ K min}^{-1}$  under flowing He ( $60 \text{ cm}^3 \text{ min}^{-1}$ ).

The H-D isotopic exchange on the supported heteropolyacid materials was also investigated by *in situ* FTIR. The sample was contacted into the infrared cell with vapor of D<sub>2</sub>O at 348 K for 10 min, and then was purged under flowing He ( $60 \text{ cm}^3 \text{ min}^{-1}$ ) at the same temperature for 30 min. Next, the evolution of the infrared signals was followed by heating the IR cell from RT to 623 K at  $10 \text{ K min}^{-1}$ .

A Nicolet Magna 550 FTIR spectrometer with a MCT detector was used to acquire the spectra ( $4 \text{ cm}^{-1}$  resolution, 100 scans). The overlapping bands, along with the measurement of peak areas, were solved using sum of lorentzian curves.

All gases were high purity grade (99.999%) and were further purified through molecular sieve (3Å) and MnO/Al<sub>2</sub>O<sub>3</sub> traps to remove water and oxygen impurities, respectively.

### 3. Results

### 3.1. Molecular Structure of Oxide Supported Wells-Dawson HPA at Theoretical “Monolayer” Coverage

Previous investigations reported by some of us demonstrated that Raman spectroscopy is a reliable tool to establish the molecular structure of bulk Wells-Dawson and Keggin type heteropolyacids<sup>15-17</sup>. Moreover, this spectroscopy allowed distinguishing between bulk HPA and a bi-dimensional layer of the heteropolyanion  $P_2W_{18}O_{62}^{6-}$  dispersed over  $TiO_2$  at various loadings<sup>11</sup>. In this context and continuing with those previous studies this section presents the investigation of the molecular structure of the oxide-supported Wells-Dawson HPA synthesized both in aqueous and organic media. Table 1 presents the HPA loading, tungsten surface density, the aqueous or organic medium of synthesis and the specific surface area of the oxide supported HPA. Additionally, Figure 1 shows the ambient Raman spectra (with the exception of 12org WDAI taken at 373 K) of those materials synthesized in aqueous and organic medium, respectively. The spectra of the bulk HPA under ambient conditions is also presented for comparison purposes.

The Raman spectra of the HPA dispersed over  $TiO_2$ ,  $SiO_2$  and  $Al_2O_3$  show a signal at 995-992  $cm^{-1}$ . In the particular case of 11aq WDTi, 11org WDTi and 13aq WDSi, that signal was observed regardless of the nature of the synthesis medium (aqueous or organic). The fluorescence of  $ZrO_2$  and  $Al_2O_3$  (subjected to ethanol during the organic synthesis) prevents the observation of any signal until further heating, as it will be described below.

The Raman signal of these oxide-supported HPA is similar to the strong one at  $998\text{ cm}^{-1}$  of the bulk heteropolyacid<sup>15</sup>, which is ascribed to the symmetric stretching vibration of the double bonded tungsten-terminal oxygen  $\nu_s(\text{W}=\text{O}_t)$  species, along with its shoulder near  $970\text{ cm}^{-1}$ . The absence of other signals evidences that neither Keggin phases (typically at  $1007\text{ cm}^{-1}$ ) nor tungsten oxide (typically at  $805\text{ cm}^{-1}$ ) are somehow produced during the synthesis. In principle, the Wells-Dawson HPA does not decompose when dissolved in aqueous or ethanol media or when is in contact with the oxide supports during the synthesis.

The X-ray diffraction spectra of the oxide-supported HPA showed the XRD signals of the transition metal oxides ( $\text{TiO}_2$ ,  $\text{ZrO}_2$ ,  $\text{SiO}_2$  and  $\text{Al}_2\text{O}_3$ ) and only in the particular cases of 11aq WDSi and 12aq WDAI an additional signal at  $2\theta \sim 7^\circ$  was detected (see figure 2S in the Supplementary Information). The low intensity and resolution of this signal, ascribed to bulk phosphotungstic heteropolyacid  $\text{H}_6\text{P}_2\text{W}_{18}\text{O}_{62}\cdot x\text{H}_2\text{O}$ , is an indication of the poor crystallinity of the HPA<sup>18</sup>. These results are in accordance with the observations reported by Bielański et al.<sup>10</sup> and Marci et al.<sup>19</sup> of phosphotungstic Keggin and Wells-Dawson heteropolyacids dispersed over transition metal oxides supports at loadings corresponding to 0.3-11 and 11-25  $\text{W}_{\text{atom}}/\text{nm}^2$ , respectively. The fact that the presence of crystals is detected in the Raman spectra is somehow an evidence of the size of the crystals since it is well known that such spectroscopy is able to detect nanocrystals of less than 4 nm of size.<sup>20</sup>

### 3.2. Evolution of the Molecular Structure of Oxide Supported Wells-Dawson HPA Upon Heating

Figures 2 to 5 present the *in situ* temperature-programmed Raman spectra during the calcinations of the oxide-supported HPA series synthesized in aqueous media. Additionally, the spectra of the materials synthesized in organic media are presented in the Supplementary Information section (figures 7S, 8S and 9S). The stability of the Wells-Dawson phosphotungstic heteropolyacid dispersed over silica oxide has been extensively reported in the literature; therefore, only the material synthesized in aqueous media is presented in this investigation<sup>1,3,4,9,10</sup>.

The Supplementary Information shows the Raman analyses of the bare oxide supports along with the bulk Wells-Dawson heteropolyacid under similar thermal treatments, showing now significant change. In addition, the positions of the Raman signals of the transition metal oxides do not interfere with the ones belonging to the heteropolyacid species, which ensures the reliability of the discussion presented in this section. Although, the bulk Wells-Dawson heteropolyacid has already been reported by some of us it is important to remind here the evolution of this structure under heating in order to discuss the oxide-supported systems<sup>15</sup>.

Figures 2, 4 and 5 show a signal at 992-997  $\text{cm}^{-1}$  attributed to the asymmetric stretching vibration of the double bonded tungsten-oxygen bonds  $\nu_s(\text{W}=\text{O}_t)$  of the fully hydrated HPA structure<sup>15</sup>. This signal is observed in all the

materials at RT with the exception of 11aq WDZr and 11org WDZr (see figures 3 and 8S in Supplementary Information).

The increase of the temperature from 373 K to 523 K progressively shifts the band at 992-997  $\text{cm}^{-1}$  towards 1004-1010  $\text{cm}^{-1}$  (figures 2, 4 and 5). A signal at 1019-1021  $\text{cm}^{-1}$  dominates the spectra above 523 K and up to 773 K. Previous investigation of some of us demonstrated that the shift of the Raman bands is associated with the gradual dehydration of the HPA<sup>11, 15</sup>. In fact, the water molecules of the HPA structure  $\text{H}_6\text{P}_2\text{W}_{18}\text{O}_{62}\cdot x\text{H}_2\text{O}$  are associated with protons forming large protonated water clusters  $\text{H}^+(\text{H}_2\text{O})_n$  which degrade to  $\text{H}_3\text{O}^+$  and  $\text{H}_5\text{O}_2^+$  at 473 K and finally to Brønsted acid sites<sup>6</sup>. In this context, the spectra of 11aq WDTi (Figure 2), 11org WDTi (Figure 7S), 12aq WDAI (Figure 4), 12org WDAI (Figure 9S) and 13aq WDSi (Figure 5) show the coexistence of two signals at 990-1000 and 1018-1021  $\text{cm}^{-1}$  in the 473-673 K range. This observation suggests the coexistence of fully and partially hydrated heteropolyacid domains during the gradual dehydration of the HPA structure.

No spectra could be recorded for 11aq WDZr and 11org WDZr below 523 K due to strong fluorescence background as discussed before (see Figures 3 and 8S). However, a Raman band at 1019  $\text{cm}^{-1}$  is apparent at 523 K. The presence of an additional signal at 806  $\text{cm}^{-1}$  is observed above 723 K (see Figure 6), which evidences the decomposition of the HPA towards tungsten trioxide.

The next section provides additional evidences on the dehydration process of the oxide-supported Wells-Dawson heteropolyacid through the

investigation of the evolution of the water molecules associated to that structure.

### 3.3. Evolution of the Structural Water Molecules of the HPA Upon Heating

Figures 7 to 9 show the *in situ* temperature programmed infrared spectra obtained during the calcination of the oxide-supported HPA. This investigation was performed exclusively on the materials synthesized in aqueous media since their molecular structure is similar to the ones synthesized in organic media.

The spectra of 11aq WDZr (Figure 7) and 12aq WDAI (Figure 8) show the characteristic infrared signal at about 1086-1092  $\text{cm}^{-1}$  assigned to the vibration of P-O bond of the Wells-Dawson structure that remains unaltered with the increasing temperature<sup>12, 18</sup>. This signal is not observed in the IR spectra of the  $\text{SiO}_2$  supported HPA due to the intense absorption of this oxide support below 1500  $\text{cm}^{-1}$ . The appearance of this signal in the infrared spectra provides further evidences of the presence of bulk HPA on the surface of oxide supports, in line with Raman spectra. This observation is relevant in the case of the  $\text{ZrO}_2$ -supported HPA (aqueous and organic preparation) since neither the Raman spectra nor the X-Ray analysis were conclusive.

In contrast with the phosphorous-oxygen species, the signals at 1628-1634  $\text{cm}^{-1}$  and the broad one centered at about 3400  $\text{cm}^{-1}$  are perturbed upon increasing temperature. These vibrations are ascribed to the bending modes  $\delta(\text{O-H})$  of adsorbed molecular  $\text{H}_2\text{O}$  and the stretching of the O-H species,

respectively <sup>21, 22</sup>. Additionally, another signal at  $1425\text{ cm}^{-1}$  that corresponds to the vibration of water molecules adsorbed on the material is observed in the infrared spectra of 11aq WDZr (see Figure 7).

The Figures 7 and 9 show that the signal at  $\sim 1630\text{ cm}^{-1}$  weakens in the 353 - 373 K range and is replaced by another band at about  $1614\text{ cm}^{-1}$  that is observed at high temperatures. On the other hand, the signal at  $\sim 3400\text{ cm}^{-1}$ , corresponding to the vibration of the O-H bonds, decreases in the interval ranging from room temperature to 623 K. In the particular case of 12aq WDAI both the signals at  $1634\text{ cm}^{-1}$  and  $3512\text{ cm}^{-1}$  are somehow more stable since are observed up to 473 K.

A similar behavior was previously observed upon dehydration of 11aq WDTi <sup>11</sup>. In this context, the temperature-programmed infrared spectra revealed that the signal at  $1623\text{ cm}^{-1}$  is replaced by a new one at  $1588\text{ cm}^{-1}$ , which remains stable up to 723 K. Moreover, the temperature-programmed infrared analyses of the bare oxide supports under similar thermal treatments evidence that none of the oxide supports possesses the signal at  $1614\text{ cm}^{-1}$ , which is characteristic of the supported HPA materials (see Supplementary Information).

The observations described above indicate that the molecules of water associated with the HPA structure possess characteristic infrared signals, which is in agreement with previous findings in salt hydrates, carborane acids and the Keggin type HPA as will be discussed in the following sections.

### 3.4. Further Evidences on the Nature of the IR Signals of Water Molecules

The Figure 10 shows the infrared spectra of 11aq WDTi under vacuum at 303 K before exposure to D<sub>2</sub>O; after exposure to D<sub>2</sub>O for 1 and 2 minutes and after evacuation at 348 K. The spectra at 303 K show the characteristic signal at 1080 cm<sup>-1</sup> assigned to the P-O bond vibration in the Wells-Dawson structure. Additionally, the signals corresponding to the bending  $\delta(\text{O-H})$  and stretching  $\nu(\text{O-H})$  vibrations of O-H species at 1623 cm<sup>-1</sup> and ~3244 cm<sup>-1</sup>, respectively, are also present. The spectra of the sample in contact with D<sub>2</sub>O vapor for 1 and 2 min at 348 K and then evacuated shows the shift of the signals characteristic of H<sub>2</sub>O by signals characteristic of  $\delta(\text{O-D})$  vibrations at 1193 cm<sup>-1</sup> and  $\nu(\text{O-D})$  vibrations at 2500 cm<sup>-1</sup> as a consequence of the hydrogen-deuterium exchange. The observed shift of the bending vibration of the O-H species from 1623 cm<sup>-1</sup> to 1193 cm<sup>-1</sup> of the bending vibration of the O-D species is in agreement with the expected one<sup>16</sup>.

On the other hand, the Figure 11 shows the *in situ* TP-IR spectra of the isotopically exchanged 11aq WDTi upon temperature-programmed desorption. The spectra show that the signals belonging to the bending and stretching vibrations of the oxygen-deuterium bond (at 1193 cm<sup>-1</sup> and 2500 cm<sup>-1</sup>, respectively) disappear in the interval from 373 to 623 K during heating.

The fact that the signal at 1193 cm<sup>-1</sup> originates from the exchange of the one originally at 1623 cm<sup>-1</sup> and that both disappear due to the dehydration of the material provides further evidences of assignments discussed in the previous section.

#### 4. Discussion

Polar molecules such as H<sub>2</sub>O, NH<sub>3</sub>, amines and alcohols not only adsorb on the external structure of heteropoly-compounds, but they also diffuse inside the structure interacting with bonded protons forming either protonated monomers or protonated clusters<sup>7,23,24</sup>. Previous reports by Bielański et al. on the adsorption-desorption of ethanol on the phosphotungstic Wells-Dawson heteropolyacid demonstrated that alcohols form protonated C<sub>2</sub>H<sub>5</sub>OH<sub>2</sub><sup>+</sup> species inside the HPA structure<sup>8,24</sup>. Furthermore, the ethoxonium ions replace the crystallization water creating hydrogen bonds between HPA anions. Interestingly, the present investigation demonstrates that neither the molecular structure nor the thermal stability of the heteropolyacid are perturbed due to the synthesis in organic media although it is expected that the alcohol become part of the pseudo-liquid region of the HPA.

It is extensively reported that the degree of hydration has an important role on the stability and catalytic performance of the heteropoly-compounds. The series of oxide-supported Wells-Dawson heteropolyacids screened in the present investigation evidence that the progressive desorption of structural water molecules does not lead to the HPA decomposition, which remains stable up to 773 K. In fact, the water molecules associated with the HPA structure (and in turn with the proton species) show distinctive infrared signals depending on the temperature. The signals near 3400 cm<sup>-1</sup> and within the 1623-1634 cm<sup>-1</sup> range are attributed to the stretching vibration  $\nu(\text{OH})$  and  $\delta(\text{H}_2\text{O})$ , respectively, of the large water clusters H<sup>+</sup>(H<sub>2</sub>O)<sub>n</sub> as discussed before. The partial desorption of water molecules begins at 353 K with the decrease and

further disappearance of both signals. This observation correlates with the literature regarding the genesis of the Zundel ion  $\text{H}_5\text{O}_2^+$  in condensed phases<sup>22, 25, 26</sup>. The Zundel ion has been detected in strong acids and is described as a proton possessing a short, strong, low barrier H-bond with two molecules of water  $\text{H}(\text{solvent})_2^+$  forming a disolvated species<sup>26</sup>. The term SSLB H-bond was coined due to the low energetic barrier for the proton species to move within an interval in the oxygen-hydrogen-oxygen bond that has been proved through theoretical calculations. Actually, the disappearance of the infrared signals belonging to the stretching  $\nu(\text{OH})$  and bending  $\delta(\text{H}_2\text{O})$  vibrations are a consequence of the delocalization of the  $\text{H}^+$  arising from the formation of the Zundel ion. Additionally new signals at  $1614\text{ cm}^{-1}$  and  $1428\text{ cm}^{-1}$  that have been associated with the  $\text{H}_5\text{O}_2^+$  species are also detected in the present contribution<sup>22, 25</sup>.

These distinctive vibrations of water molecules agree with the fact that molecules or ions linked by bonds of different strength possess different vibrational modes<sup>27</sup>. This is the case of the  $[\text{Zr}_4(\text{OH})_8(\text{H}_2\text{O})_{16}]^{8+}$  compound<sup>28</sup>, which presents infrared signals that belongs to coordinatively bound water molecules; tetrahedrally coordinated lattice water dimers at  $1620\text{ cm}^{-1}$  and strongly H-bonded lattice water accommodating hydrated protons at  $1705$  and  $1666\text{ cm}^{-1}$ . The Keggin anions  $\text{PW}_{12}\text{O}_{40}^{6-}$  (similarly to the Wells-Dawson ones) are hydrated and possess a network of hydrogen bonds connecting them. In this context, the hexahydrate Keggin anions are separated by  $\text{H}_5\text{O}_2^+$  units that possess a well-defined infrared signal at  $1732\text{ cm}^{-1}$  according to the investigation of Herring and McCormick<sup>29</sup>. This signal was assigned to the

bending vibration of the bond between an oxygen species of the HPA and a hydrogen atom of the water molecule  $\delta(\text{O-H}_w)$ . Again, similarly to our observation that signal readily disappears near 623 K.

Previous investigations reported by Sambeth et al.<sup>6,7</sup> demonstrated that bulk phosphotungstic Wells-Dawson heteropolyacid loses 17 water molecules in the 339-343 K range, five additional molecules of water desorb in the 370 - 387 K range and the last two molecules are released above 581-591 K. These observations and the shifts of the Raman modes ascribed to the  $\nu_s(\text{W=O})$  stretching vibration allows correlating the dependence of the molecular structure-water content with the temperature. In this context, the Raman signal of the fully hydrated HPA is observed near  $994\text{ cm}^{-1}$  and its 24 crystallization water molecules vibrate at  $1623\text{-}1634\text{ cm}^{-1}$  in the infrared spectra as discussed before. Above 373 K and up to 573 K, the partially hydrated structure shows a Raman signal at about  $1004\text{-}1010\text{ cm}^{-1}$ . Above 573 K, the hydroxylated structure possessing Brønsted acid sites shows a signal at  $1019\text{-}1020\text{ cm}^{-1}$ . The influence of the degree of hydration on the Raman shift have also been observed in the vanadyl  $\text{V=O}$  mode of vanadia/titania catalysts both at low and high vanadia loading<sup>30, 31</sup>. Both theoretical and experimental evidences allowed demonstrated that the redshift of the  $\text{V=O}$  and  $\text{V-O-V}$  modes upon exposure to humidity and decreasing temperature was associated to a progressive interaction with water molecules. The authors attributed the shift of the vanadyl bond vibration from  $1029\text{-}1021\text{ cm}^{-1}$  towards  $1013\text{-}1006\text{ cm}^{-1}$  to the closer interaction of such species with hydroxyl groups or water molecules with the formation of hydrogen bonds that in turn forms polyvanadates. Similarly to this

observation, our investigation shows the shift of the vibration of the tungsten-oxygen species coordinated to water clusters  $W=OH^+(H_2O)_n$  at  $994\text{ cm}^{-1}$ , towards  $1004\text{-}1010\text{ cm}^{-1}$  for  $W=OH^+(H_2O)_2$  and finally to  $1019\text{-}1020\text{ cm}^{-1}$  for  $W=OH$  and/or  $W=O$  species.

This investigation assumes that the oxide-supported HPA catalysts investigated in this study possess the maximum dispersion limit or the so called, “theoretical monolayer coverage” of the phosphotungstic heteropolyacid on the oxide supports, being this assumption valid for both, aqueous and organic media impregnation methods. The amount of  $P_2W_{18}O_{62}^{-6}$  Wells-Dawson heteropolyanions was calculated considering the dimensions of the anion reported in the literature<sup>6,9,10,14</sup>. According to the crystallographic data, the heteropolyanion is an elliptic molecule with maximum diameter of  $20\text{ \AA}$  and minimum diameter of  $10\text{ \AA}$ . Then, the heteropolyanion possesses  $1.57\times 10^{-18}\text{ m}^2$  per molecule if an elliptical projection over the oxide support is considered. Therefore one mole of molecules of the HPA would occupy an area equals to  $196.8\text{ m}^2/\text{g}$  as presented in the experimental section. On the other hand, if a circular (a circle with  $10\text{ \AA}$  of diameter) projection of the HPA over the oxide support is considered then the heteropolyanion would possess  $7.85\times 10^{-19}\text{ m}^2$  per molecule and  $98.4\text{ m}^2/\text{g}$ . In this particular situation, the maximum dispersion loadings would even be higher than the presented above. It should be noted that those assumptions stand on the idea the HPA units locate on the oxide support like tiles on a floor, and do not consider the chemical binding between the supported HPA units and the surface sites of the support, typically hydroxyl groups<sup>32, 33</sup>.

Previous investigation on a series of TiO<sub>2</sub>-supported Wells-Dawson HPA at various loadings must be considered in order to obtain more insights on the actual molecular structure of the HPA molecules dispersed on transition metals oxide supports <sup>11</sup>.

The materials with low loading (from 1.7 to 2.3  $W_{\text{atoms}}/\text{nm}^2$ ) show a unique Raman signal centered at 1002  $\text{cm}^{-1}$  (see figure 14S in Supplementary Information). Previous investigations reported by Bielański et al. demonstrated that the Wells-Dawson HPA formed islands of nanocrystals (5 nm size) when dispersed over TiO<sub>2</sub> even at loadings as low as 1  $W_{\text{atom}}/\text{nm}^2$  <sup>10</sup>. The thickness of such crystals corresponds to three to four layers of P<sub>2</sub>W<sub>18</sub>O<sub>62</sub><sup>6-</sup> anions. Therefore, according to that results and our observation it is possible to relate the Raman signal at 1002  $\text{cm}^{-1}$  to well dispersed nanocrystals of the HPA over the oxide support. The materials with 4.0 to 8.5  $W_{\text{atoms}}/\text{nm}^2$  showed that the signal at 1002  $\text{cm}^{-1}$  shifted towards 1005-1008  $\text{cm}^{-1}$  and the appearance of a vibration at ~ 1020  $\text{cm}^{-1}$  (see figure 14S in Supplementary Information). This last one dominates the spectra along with a low intensity band at 998  $\text{cm}^{-1}$  above 8.5  $W_{\text{atoms}}/\text{nm}^2$ . These Raman signals (1020  $\text{cm}^{-1}$  and 998  $\text{cm}^{-1}$ ) are similar to the ones observed in the bulk HPA calcined *in situ* at 573 K as discussed above (see Supporting Information) <sup>15, 34</sup>. The materials 11aq WD/Ti, 11org WDTi and 13aq WDSi calcined *in situ* at 573 K show the signals at 1019-1020  $\text{cm}^{-1}$  and 994-1004  $\text{cm}^{-1}$ . Additionally, the Raman spectra of 11aq WDZr, 11org WDZr, 12 aq WDAI and 12org WDAI present the signal at 1019-1020  $\text{cm}^{-1}$  at 573 K. These observations evidence the presence of HPA crystals on the oxide surface of all the materials synthesized in this investigation. The fact that

none of the oxide-supported HPA systems showed a Raman signal at  $1002\text{ cm}^{-1}$  and that no (or not well defined) crystals features were detected through X-Ray diffraction analyses suggest the presence of crystallites with a size distribution up to at least 5 nm, which are detectable by Raman spectroscopy but in the limit to generate an X-ray diffraction pattern.

## 5. CONCLUSION

The present investigation provides light on a series of controversial topics in the chemistry of heteropoly-compounds such as the influence of an aqueous and organic media in the molecular structure and thermal stability of supported Wells-Dawson heteropolyacid. The *in situ* temperature-programmed Raman spectroscopic analyses establishes that exposure of the heteropolyanion to aqueous or ethanol media has no effect on the molecular structure and thermal stability of the supported HPA, at least for the cases of  $\text{TiO}_2$ ,  $\text{SiO}_2$ ,  $\text{Al}_2\text{O}_3$  and  $\text{ZrO}_2$  supports.

The infrared study during the dehydration process of the HPA demonstrated that the large cluster of crystallization water molecules,  $\text{H}^+(\text{H}_2\text{O})_n$ , vibrate at  $\sim 1630\text{ cm}^{-1}$ . The removal of water molecules from the HPA structure reveals a signal at  $1614\text{ cm}^{-1}$  assigned to the dioxonium species  $\text{H}_5\text{O}_2^+$  (the Zundel ion) due to the association of two molecules of water with the protonic sites of the heteropolyacid.

A careful comparison of both *in situ* TP-Raman and *in situ* TP-IR spectra allows correlating the signals of the tungsten-oxygen bond with the water content. In this context, the Raman signal at  $994\text{ cm}^{-1}$  appears along with the

infrared signal at  $\sim 1630\text{ cm}^{-1}$  indicating a fully hydrated HPA structure. Similarly, the Raman signal in the  $1004\text{-}1017\text{ cm}^{-1}$  comes along with the infrared signal at  $1614\text{ cm}^{-1}$ , which would indicate the presence of partially hydrated species whose secondary structure is bonded by dioxonium species  $\text{H}_5\text{O}_2^+$ . Finally the Raman signal at  $1018\text{-}1020\text{ cm}^{-1}$  is an indicative of a hydroxylated HPA structure.

The spectroscopic evidences suggest that the “monolayer coverage” calculated with the geometric size of the Wells-Dawson heteropolyacid (typically  $11\text{ W}_{\text{atoms}}/\text{nm}^2$ ) exceeds de maximum dispersion limit loading to the formation of well defined HPA crystals. Previous reports demonstrated that the HPA forms nanocrystals at very low loadings. This observation arises the question if it is possible to obtain a unique layer of HPA units on an oxide support. The present investigation demonstrated that the Wells-Dawson heteropolyacid dispersed over  $\text{TiO}_2$  and  $\text{SiO}_2$  at loadings corresponding to  $11\text{-}13\text{ W}_{\text{atoms}}/\text{nm}^2$  unequivocally forms crystals over the oxide supports.

#### ACKNOWLEDGMENTS

The authors acknowledge the financial support of CONICET (project PIP 0083 and PIP 0278), Universidad Nacional de La Plata (project 11-X626), Argentinian ANPCYT (PICT-2012-1280) and Spanish Ministry project CTQ2011-25517. S. R. Matkovic acknowledge the Spanish Ministerio de Asuntos Exteriores y de Cooperación (MAEC) and Agencia Española de Cooperación Internacional (AECI).

## References

(1) Briand, L. E.; Baronetti, G. T.; Thomas, H. J. The State of the Art on Wells-Dawson Heteropoly-Compounds. A Review of Their Properties and Applications. *Appl. Catal. A:Gen.* **2003**, *256*, 37-50.

(2) Romanelli, G. P.; Bennardi, D.; Ruiz, D. M.; Baronetti, G.; Thomas, H. J.; Autino, J.C. A Solvent-Free Synthesis of Coumarins Using a Wells–Dawson Heteropolyacid as Catalyst. *Tetrahedron* **2004**, *45*, 8935–8939.

(3) Gustavo Pasquale, G.; Vázquez, P.; Romanelli, G.; Baronetti, G. Catalytic Upgrading of Levulinic Acid to Ethyl Levulinate Using Reusable Silica-Included Wells-Dawson Heteropolyacid as Catalyst. *Catal. Commun.* **2012**, *18*, 115-120.

(4) Bennardi, D. O.; Romanelli, G. P.; Sathicq, A. G.; Autino, J. C.; Baronetti, G. T.; Thomas, H. J.; Wells–Dawson Heteropolyacid as Reusable Catalyst for Sustainable Synthesis of Flavones. *Appl. Catal. A: Gen.* **2011**, *404*, 68-73.

(5) Li, G.; Ding, Y.; Wang, J.; Wang, X.; Suo, J. New Progress of Keggin and Wells–Dawson Type Polyoxometalates Catalyze Acid and Oxidative Reactions. *J. Mol. Catal. A: Chem.*, **2007**, *262*, 67-76.

(6) Sambeth, J. E.; Baronetti, G. T.; Thomas, H. J. A Theoretical–

Experimental Study of Wells–Dawson Acid: An Explanation of Their Catalytic Activity. *J. Molec. Catal. A: Chem.* **2003**, *191*, 35-43.

(7) Sambeth, J. E.; Romanelli, G.; Autino, J. C.; Thomas, H. J.; Baronetti, G. T. A Theoretical–Experimental Study of Wells-Dawson Phospho-tungstic Heteropolyacid: An Explanation of the Pseudoliquid or Surface-Type Behaviour. *Appl. Catal.* **2010**, *378*, 114-118.

(8) Bielański, A.; Lubańska, A.; Micek-Ilnicka, A.; Poźniczek, J. Polyoxometalates as the Catalysts for Tertiary Ethers MTBE and ETBE Synthesis. *Coord. Chem. Rev.* **2005**, *249*, 2222-2231.

(9) Baronetti, G. T.; Thomas, H. J.; Querini, C. A. Wells-Dawson Heteropolyacid Supported on Silica: Isobutane Alkylation with C4 Olefins. *Appl. Catal.* **2001**, *217*, 131-141.

(10) Poźniczek, J.; Lubańska, A.; Micek-Ilnicka, A.; Mucha, D.; Lalik, A.; Bielański, A. TiO<sub>2</sub> and SiO<sub>2</sub> Supported Wells-Dawson Heteropolyacid H<sub>6</sub>P<sub>2</sub>W<sub>18</sub>O<sub>62</sub> as the Catalyst for ETBE Formation. *Appl. Catal.* **2006**, *298*, 217-224.

(11) Matkovic, S. R.; Collins, S. E.; Bonivardi, A. L.; Bañares, M. A. Infrared and Raman Investigation of Supported Phosphotungstic Wells-Dawson Heteropolyacid. *Current Catal.* **2014**, *3*, 199-205.

(12) Matkovic, S. R.; Valle, G. M.; Gambaro, L. A.; Briand, L. E. Environmentally Friendly Synthesis of Wells–Dawson Heteropolyacids: Active Acid Sites Investigation Through TPSR of Isopropanol. *Catal. Today*, **2008**, 133-135, 192-199.

(13) Valle, G. M.; Matkovic, S. R.; Gambaro, L. A.; Briand, L. E. *Handbook of Catalysts Synthesis. The Science and Engineering of Catalyst Preparation*. J.R. Regalbuto ed., CRC Taylor & Francis, Florida-USA, **2006**.

(14) Dawson, B. The Structure of the 9(18)-Heteropoly Anion in Potassium 9(18)-Tungstophosphate,  $K_6(P_2W_{18}O_{62}) \cdot 14H_2O$ . *Acta Crystallogr.* **1953**, 6, 113-126.

(15) Matkovic, S. R.; Briand, L. E.; Bañares, M. A. Investigation of the Thermal Stability of Phosphotungstic Wells-Dawson Heteropoly-Acid Through in situ Raman Spectroscopy. *Mater. Res. Bull.*, **2011**, 46, 1946–1948.

(16) Collins, S. E.; Matkovic, S. R.; Bonivardi, A. L.; Briand, L. E. Acylating Capacity of the Phosphotungstic Wells-Dawson Heteropoly Acid: Intermediate Reactive Species *J. Phys. Chem. C*, **2011**, 115, 700–709.

(17) Damyanova, S.; Gómez, L. M.; Bañares, M. A.; Fierro, J. L. G. Thermal Behavior of 12-Molybdophosphoric Acid Supported on Zirconium-Loaded Silica.

*Chem. Mater.*, **2001**, *12*, 501-510

(18) Baronetti, G.; Briand, L.; Sedran, U.; Thomas, H. Heteropolyacid-Based Catalysis. Dawson Acid for MTBE Synthesis in Gas Phase. *Appl. Catal. A: General*, **1998**, *172*, 265-272.

(19) Marci, G.; García-López, E.; Bellardita, M.; Parisi, F.; Colbeau-Justin, C.; Sorgues S.; Liotta, L. F.; Palmisano, L. Keggin Heteropolyacid  $H_3PW_{12}O_{40}$  Supported on Different Oxides for Catalytic and Catalytic Photo-assisted Propene Hydration. *Phys. Chem. Chem. Phys.* **2013**, *15*, 13329-13342.

(20) Bañares, M. A., Chapter 4: Raman Spectroscopy in *In Situ spectroscopy of Catalysts*, edited by B. M. Weckhuysen, American Scientific Publishers, **2004**.

(21) Ryczkowski, J. IR Spectroscopy in Catalysis. *Catal. Today* **2001**, *68*, 263-381.

(22) Stoyanov, E. S.; Reed, C. A. IR Spectrum of the  $H_5O_2^+$  Cation in the Context of Proton Disolvates  $L-H^+-L$ . *J. Phys. Chem. A* **2006**, *110*, 12992-13002.

(23) Micek-Ilnicka, A.; Lubańska, A.; Mucha, D. The Effect of Proton Hydration in Wells-Dawson and Keggin Type Heteropolyacids on their Catalytic Activity in

Gas Phase ETBE Synthesis. *Catal. Lett.* **2009**, *127*, 285-290.

(24) Bielański, A.; Lubańska, A. FTIR Investigation on Dawson and Keggin Type Heteropolyacids: Dehydration and Ethanol Sorption. *J. Mol. Catal. A: Chem.* **2004**, *224*, 179-187.

(25) Stasko, D.; Hoffmann, S. P.; Kim, K-C.; Fackler, N. L. P.; Larsen, A. S.; Drovetskaya, T.; Tham, F. S.; Reed, C. A.; Rickard, C. E. F.; Boyd, P. D. W.; Stoyanov, E. S. Molecular Structure of the Solvated Proton in Isolated Salts. Short, Strong, Low Barrier (SSLB) H-bonds. *J. Am. Chem. Soc.* **2001**, *124*, 13869-13876.

(26) Reed, C. A. Myths about the Proton. The Nature of H<sup>+</sup> in Condensed Media. *Acc. Chem. Res.* **2013**, *46*, 2567-2575.

(27) Lutz, H. D.; Haeuseler, H. Infrared and Raman Spectroscopy in Inorganic Solids Research. *J. Mol. Struct.* **1999**, *511-512*, 69-75.

(28) Scholz, J.; Scholz (nee Böhme), K.; McQuillan, A. J. In Situ Infrared Spectroscopic Analysis of the Water Modes of [Zr(OH)<sub>8</sub>(H<sub>2</sub>O)<sub>16</sub>]<sup>8+</sup> During the Thermal Dehydration of ZrOCl<sub>2</sub>·8H<sub>2</sub>O. *J. Phys. Chem. A* **2010**, *114*, 7733-7741.

(29) Herring, A. M.; McCormick, R. L. In -Situ Infrared Study of the Absorption of Nitric-Oxide by 12-Tungstophosphoric Acid. *J. Phys. Chem. B* **1998**, *102*, 3175-3184.

(30) Lewandowska, A. E.; Calatayud, M.; Tielens, F.; Bañares, M. A. Dynamics of Hydration in Vanadia-Titania Catalysts at Low Loading: A Theoretical and Experimental Study. *J. Phys. Chem. C* **2011**, *115*, 24133-24142.

(31) Lewandowska, A. E.; Calatayud, M.; Tielens, F.; Bañares, M. A. Hydration Dynamics for Vanadia/Titania Catalysts at High Loading: A Combined Theoretical and Experimental Study. *J. Phys. Chem. C* **2013**, *117*, 25535-25544.

(32) Roark R. D.; Kohler S. D.; Ekerdt J. G. Role of Silanol Groups in Dispersion Mo(VI) on Silica. *Catal. Lett.* **1992**, *16*, 71-76.

(33) Roark R. D.; Ekerdt J. G.; Kim D. S.; Wachs I. E. Monolayer Dispersion of Molybdenum on Silica. *Catal. Lett.* **1992**, *16*, 77-83.

(34) Ross-Medgaarden, E. I.; Wachs, I. E. Structural Determination of Bulk and Surface Tungsten Oxides with UV-Vis. Diffuse Reflectance Spectroscopy and Raman Spectroscopy. *J. Phys. Chem. C* **2007**, *111*, 15089-15099.

Legends of the figures

**Figure 1.** Raman spectra (at R.T.) of 11aq WDTi, 11org WDTi, 11aq WDZr, 11org WDZr, 12aq WDAI (spectra taken at 373 K), 12aq WDAI, 13aq WDSi and bulk phosphotungstic Wells-Dawson heteropolyacid  $H_6P_2W_{18}O_{62} \cdot 24H_2O$

**Figure 2.** *In situ* TP-Raman spectra upon heating from R.T. towards 773 K of 11aq WDTi

**Figure 3.** *In situ* TP-Raman spectra upon heating from R.T. towards 773 K of 11aq WDZr

**Figure 4.** *In situ* TP-Raman spectra upon heating from R.T. towards 773 K of 12aq WDAI

**Figure 5.** *In situ* TP-Raman spectra upon heating from R.T. towards 773 K of 13aq WDSi

**Figure 6.** Comparison of the Raman spectra of 11aq WDZr calcined at 673 K (amplified  $10^8$  times), 723 K and 773 K; and 11org WDZr calcined at 723 K and 773 K (amplified  $10^8$  times)

**Figure 7.** *In situ* TP-infrared spectra upon heating from R.T. towards 723 K of 11aq WDZr

**Figure 8.** *In situ* TP-infrared spectra upon heating from R.T. towards 723 K of 12aq WDAI

**Figure 9.** *In situ* TP-infrared spectra upon heating from R.T. towards 723 K of 13aq WDSi

**Figure 10.** *In situ* IR spectra of 11aq WDTi in the isotopic exchange of H<sub>2</sub>O for D<sub>2</sub>O

**Figure 11.** *In situ* IR spectra during the temperature programmed desorption of the isotopically exchanged 11aq WDTi

FIGURE 1

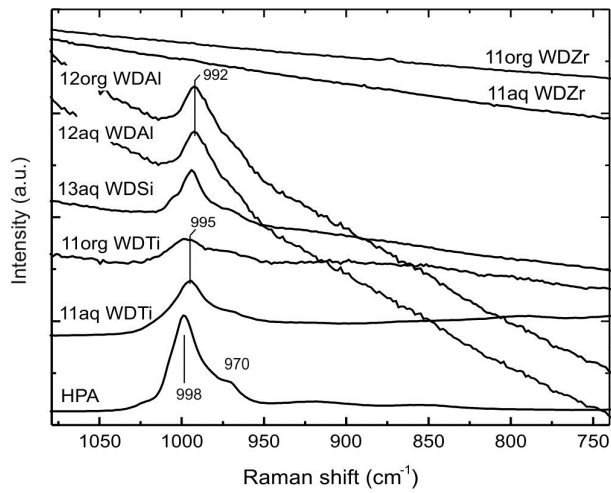


FIGURE 2

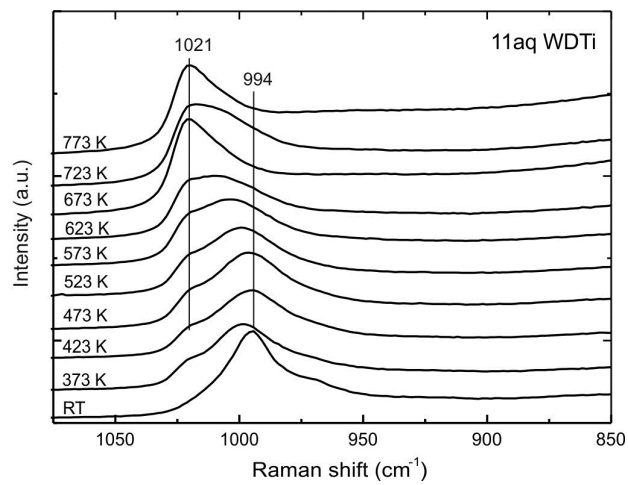


FIGURE 3

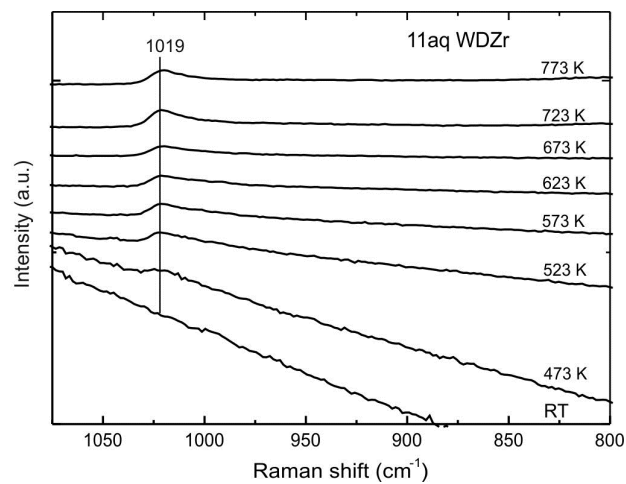


FIGURE 4

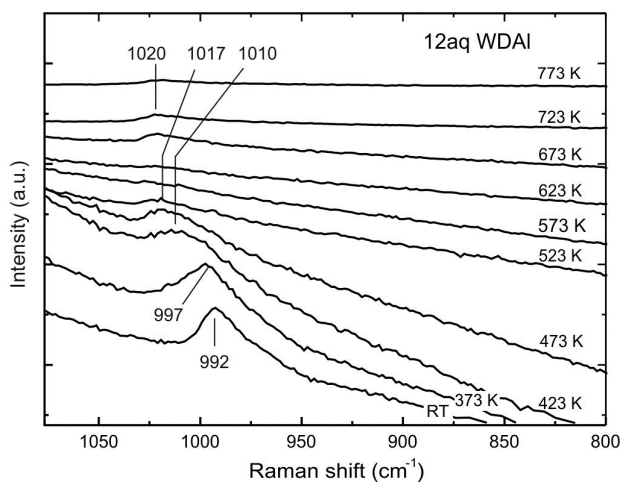


FIGURE 5

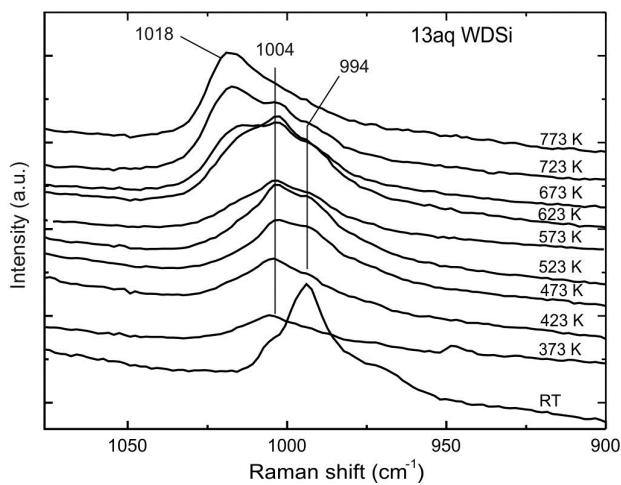


FIGURE 6

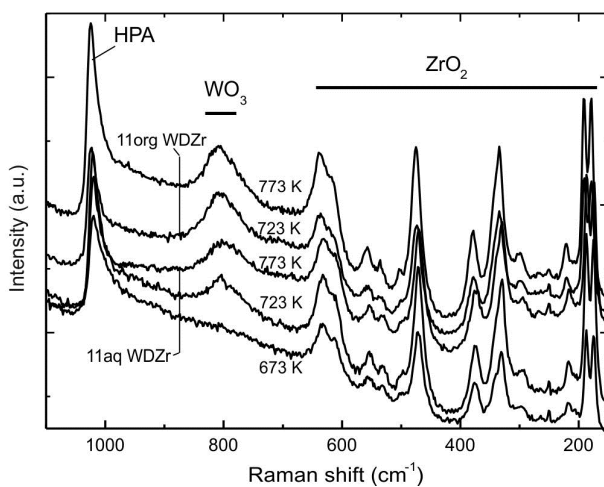


FIGURE 7

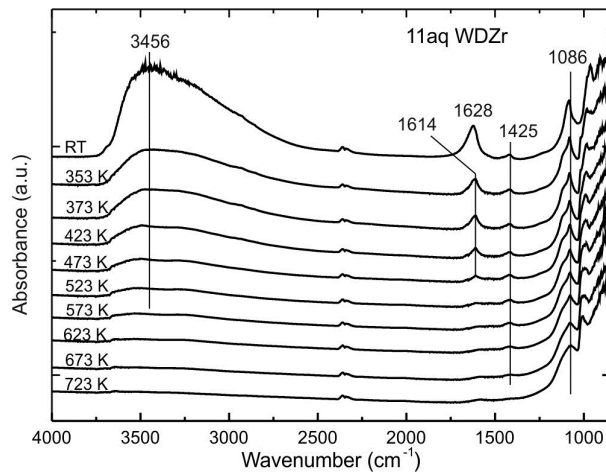


FIGURE 8

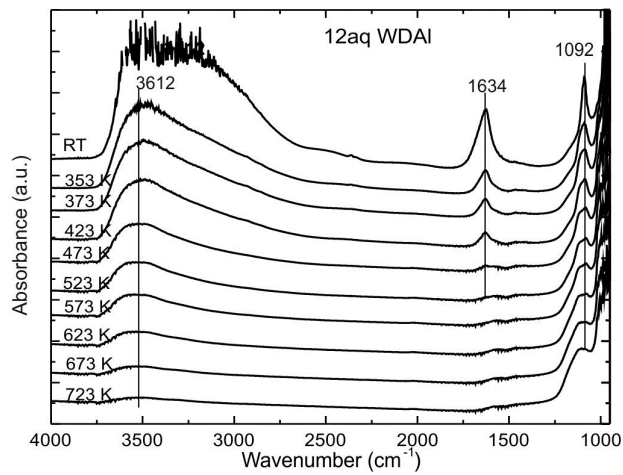


FIGURE 9

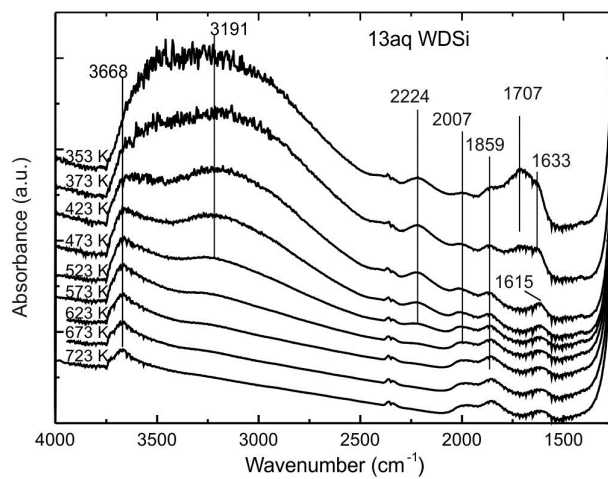


FIGURE 10

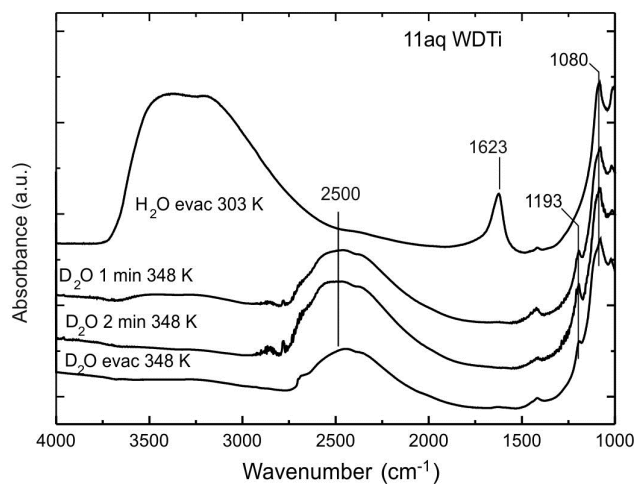
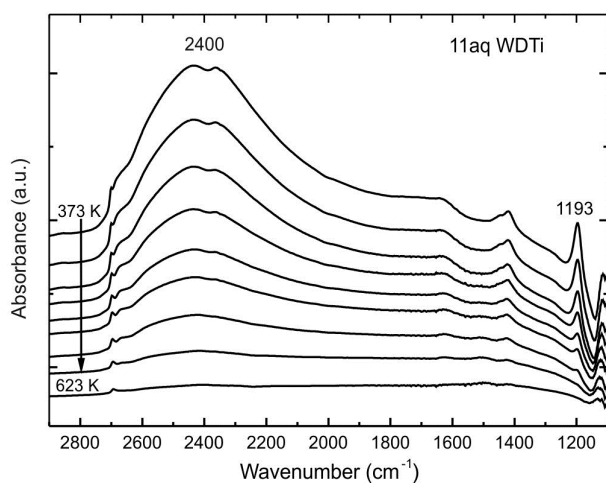


FIGURE 11



**Table 1.** HPA loading and specific surface area of the oxide supported Wells Dawson heteropoly acid synthesized in aqueous and organic media.

Oxide support	HPA loading wt. %	W surface density atoms/nm <sup>2</sup>	Aqueous/organic synthesis	S <sub>BET</sub> (m <sup>2</sup> /g)
TiO <sub>2</sub>	19	11	aqueous	49.9
	19	11	organic	41.7
SiO <sub>2</sub>	66	13	aqueous	277.3
ZrO <sub>2</sub>	13	11	aqueous	41.2
	13	11	organic	40.9
Al <sub>2</sub> O <sub>3</sub>	33	12	aqueous	92.4
	33	12	organic	89.6

|